

## Detecting non-uniform phosphorus distribution in ancient Indian iron by colour metallography

P. Piccardo<sup>1</sup>, M. G. Ienco<sup>1</sup>, R. Balasubramaniam<sup>2,\*</sup> and P. Dillmann<sup>3</sup>

<sup>1</sup>DCCI, Università di Genova, Via Dodecaneso 31, Genova I 16 146, Italy

<sup>2</sup>Department of Materials and Metallurgical Engineering, Indian Institute of Technology, Kanpur 208 016, India

<sup>3</sup>LRC CEA DSMO1-27, CNRS IRAMAT UMR5060, UTBM, and Laboratoire Pierre Süe CEA/CNRS, CE Saclay 91191 Gif sur Yvette Cedex, France

**The use of Klemm etchant for revealing the non-homogeneous distribution of phosphorus in ancient archaeological iron by colour metallography has been demonstrated. The ‘ghost’ structures produced by this etchant have also been addressed.**

ONE of the characteristic features of ancient Indian iron is the relatively high concentration of phosphorus (P) in solid solution<sup>1</sup>. In fact, phosphoric iron (typically containing 0.05 to 0.5 wt% P and less than 0.1 wt% carbon) is generally found in archaeological sites from different parts of the world, attesting to its widespread use in ancient times<sup>2</sup>. In some cases, higher carbon contents are encountered in ancient iron. Phosphorus can be present in solid solution in the iron matrix or in fixed (i.e. combined) form as phosphates in the entrapped slag inclusion. The slag inclusions in ancient Indian iron are composed mainly of fayalite (Fe<sub>2</sub>SiO<sub>4</sub>), along with wüstite and glassy phases<sup>3</sup>. These entrapped inclusions are present in ancient Indian iron because iron was extracted from the ore by the direct reduction process. In this process, the ore was directly reduced in the solid state by charcoal to produce almost pure iron. The solid-state reduced bloom, from the bloomery furnace, was hammered immediately after removal from the furnace in order to squeeze out the still-liquid slags present in the pores of the hot bloom. As it was impossible to remove the slag completely, some of it was invariably retained in the pancake on cooling down the hammered bloom. This is the origin of entrapped slag inclusions in ancient Indian iron, in general. Iron alloys obtained by the solid-state reduction route are called wrought iron. The process of ancient iron-making has sometimes been described as a sinter-forging operation<sup>4</sup>. As limestone was not used in the charge of the ancient Indian bloomery furnaces, this resulted in a higher amount of P retention in the extracted iron because the dephosphorization efficiency of fayalite/wüstite/phosphate slags is generally lower than CaO-bearing slags<sup>1</sup>. It is, therefore, not inappropriate to term ancient Indian iron as phosphoric iron.

The presence of a relatively high amount of P in ancient Indian iron results in several interesting effects. The superior atmospheric corrosion resistance of ancient Indian iron has been attributed to the high P content<sup>5</sup>. The surface processes involved in protective film formation in P-bearing wrought iron are amply evident in the example of the famous Delhi iron pillar<sup>6</sup>. The mechanism for protective film formation on modern P-bearing weathering steel has also been worked out<sup>7,8</sup>. The role of P could have also been important in the sinter-forging operations. The range of compositions normally observed in ancient iron<sup>1,3,9</sup> is between 0.2 and 0.8 wt% P. For example, according to the Fe–P phase diagram, for 0.4 wt% P, the equilibrium phases in the temperature range of 1100 to 1300°C are a mixture of two solid phases: alpha iron (ferrite) and gamma iron (austenite). The Fe–P phase diagram and the associated phase transformations have been discussed in detail elsewhere<sup>10</sup>. The austenite phase, possessing a lower solubility for P, will form at the grain boundaries. The presence of this austenite phase at the grain boundaries might have assisted sinter-forging operations because of its ductile nature.

The present communication describes the application of colour metallography in understanding P distribution in ancient iron. The phosphorus distribution in archaeological iron is non-uniform due to microsegregation that occurs during the extraction process<sup>11,12</sup>. Macro-segregation is not realized because the iron is never in the liquid state. In phosphoric iron, metallographic etching with nital provides the so-called ‘ghosting’ effect, a wrinkled or watery appearance of the ferritic grains. The sharply defined nature of the boundaries observed in the ‘ghost’ structure is due to high-temperature metallurgical transformations (ferrite to austenite) and these have been discussed in detail elsewhere<sup>13</sup>. It has been earlier shown that the Oberhoffer etchant (500 cc distilled water, 500 cc ethanol, 0.5 g stannous chloride, 1 g cupric chloride, 30 g ferric chloride and 50 cc nitric acid) can be successfully employed to reveal P microsegregation in archaeological iron<sup>14</sup>. The etch deposits Cu on regions low in P and therefore these regions appear dark during observation in the optical microscope. Regions high in P appear bright because of lower Cu deposition. This etchant has been used to study the austenite–ferrite and ferrite–austenite transformation in phosphoric iron<sup>13</sup>, and micro- and macrosegregation of P in archaeological iron<sup>15–18</sup>.

A typical ancient Indian iron obtained from the Gupta temple at Deogarh would be specifically addressed. Deogarh is situated in western Uttar Pradesh and the nearest city is Jhansi. The Gupta temple at Deogarh has been tentatively dated to the 6th century AD<sup>19,20</sup>. The artistically meritorious stone sculptures from this temple have been critically acclaimed and well reported<sup>19,20</sup>. However, there is no mention of the large number of iron clamps that were used in holding together the stone blocks that formed the structure. Generally, art historians and archaeologists tend

\*For correspondence. (e-mail: bala@iitk.ac.in)

to ignore the utility and presence of simple iron objects like clamps in their studies. The iron clamp utilized in the present investigation was obtained from the temple substructure. (A picture of the clamp is provided in Figure 1, ref. 10.) The clamp was found exposed to atmosphere when it was extracted for scientific studies. The non-uniform P distribution in this iron would thus be understood.

The microstructure of the iron clamp was obtained after sectioning it. The composition of the sample, determined from a specimen cut from the clamp, was determined by wet chemical analysis to be 0.30% P, 0.21% Si, 0.18% Al, 0.11% Ni, 0.024% C and 0.013% S. In the unetched condition, elongated slag inclusions were revealed. They were distributed unevenly with no apparent regularity. In some regions, the volume fraction of the slag inclusions was higher than in other locations. This heterogeneous distribution of entrapped slag inclusions is also another typical feature of ancient iron microstructures. Upon etching the polished surfaces with nital, microstructures typical of ancient Indian iron<sup>3,21,22</sup> were revealed. The structure of the wrought iron was essentially ferritic. This is understandable because of the low carbon content.

Generally, the regions near slag inclusions in ancient Indian iron are depleted<sup>3</sup> of P. This is due to dephosphorization by the slag. A relatively quick method to determine P depletion is by metallography. Traditionally, the etchants used for understanding P segregation are Stead's and Oberhoffer's reagents<sup>13,14</sup>. Both these etchants reveal local phosphorus segregation by depositing copper in regions low in P. The microstructure of Deogarh iron after etching in Oberhoffer etchant showed areas that are depleted in P near the slag inclusions (Figure 1). The variation in P concentration was observed by the different grades of grey coloration, with the regions low in P appearing darker than those high in P, which appeared light coloured (Figure 1 *a* and *b*).

The microstructure of Deogarh iron was etched using Klemm's I reagent (50 ml saturated aqueous sodium thio-sulphate and 1 g potassium meta-bisulphide). Typical etching time for ancient iron ranged between 30 and 90 s. This tint etchant has been recommended to colour the ferrite grains and also for revealing the segregation of P in steel. Here it has been employed for the study of archaeological iron. The microstructural features at two regions, near slag inclusions and in the bulk of the matrix, are discussed.

A typical microstructure, obtained using secondary electrons in a scanning electron microscope (SEM) is presented in Figure 2. The presence of two elongated, entrapped slag inclusions can be noted. The spot compositions at locations marked by numbers in Figure 2 were obtained from the composition analysis unit attached to the SEM. The slag composition (in wt%) at location 1 was 41.1 O, 37.8 Fe, 9.0 Al, 7.1 Si, 2.8 Ca, 0.8 Ti, 0.7 K, 0.2 Mg and 0.5 P. Locations 2, 3 and 4 were in the iron matrix (pro-

gressing away from the slag–matrix interface) and P concentrations at these locations were 0, 0.10 and 0.28% respectively. The P content increases on moving away from the slag–metal interface. This is indicative of dephosphorization due to the slag. The same region after etching in Klemm's reagent appears as shown in Figure 3. The different coloration indicates regions of varying P content. The completely ferritic regions poor in P appear blue in colour while the regions relatively richer in P are brown/reddish in colour. Apart from revealing compositional difference, the etching also reveals the grain sizes. The blue-coloured regions surrounding the slag inclusions provide a visual representation of the dephosphorization near the entrapped slag inclusion.

The microstructures containing higher P are coloured relatively brownish-red in Figure 3. The regions of higher P content were also analysed. Two typical examples are shown in Figure 4 *a* and *b*. The P compositions in the region marked 2 (Figure 4 *a*) were lower than those in the region marked 4. Therefore, regions richer in P appear bright in the figure. The etch also revealed dark-coloured

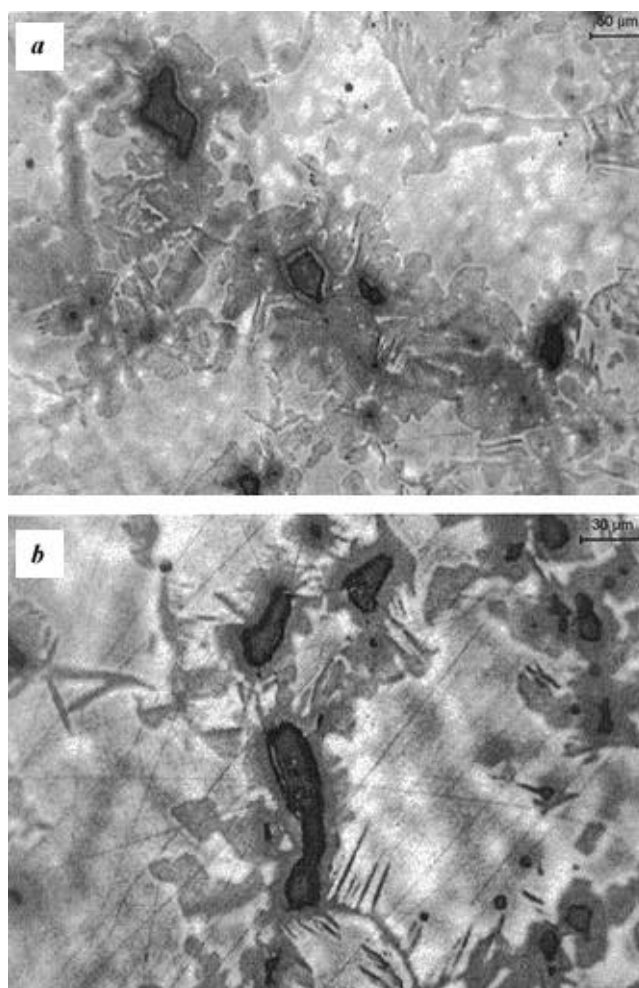


**Figure 1 a-b.** Microstructures of Gupta period iron revealed using Oberhoffer etchant. Regions depleted in P appear darker in contrast.

allotriomorphs and needle-shaped Widmanstätten structures along the grain-boundaries. It is important to understand the allotriomorphic ghost structures of the prior austenite phase along the grain-boundary regions. During high-temperature treatment (either during the extraction process or during deformation processing), the iron was in

the two-phase austenite + ferrite region (the Fe-P phase diagram exhibits a gamma loop at high temperature), such

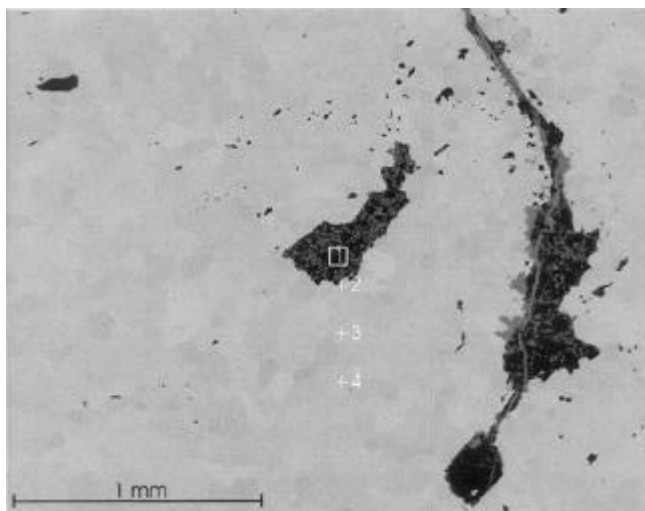


**Figure 2.** Scanning electron micrograph showing entrapped slag inclusions. Spot compositions were obtained at the marked locations.

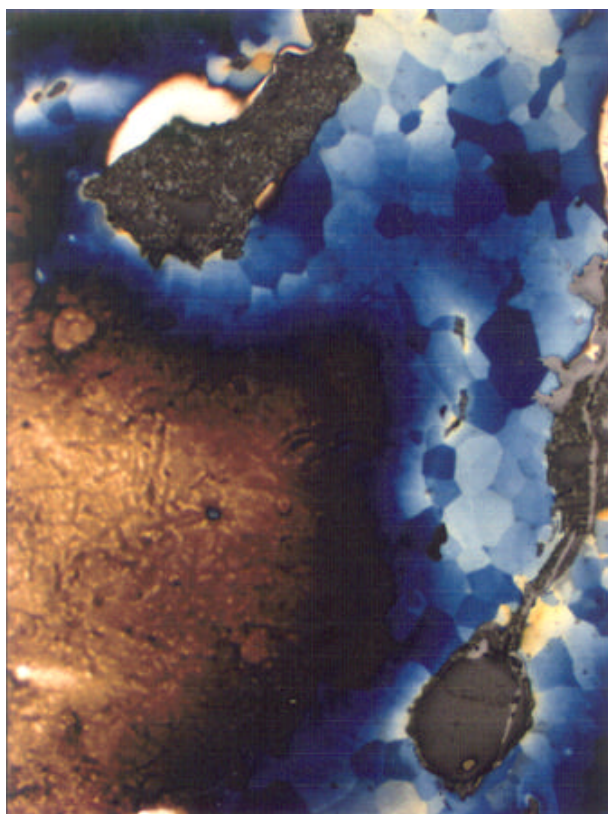


**Figure 3.** Microstructure of the same location as in Figure 2, revealed using Klemm etchant. Blue-coloured regions are those of low P content.

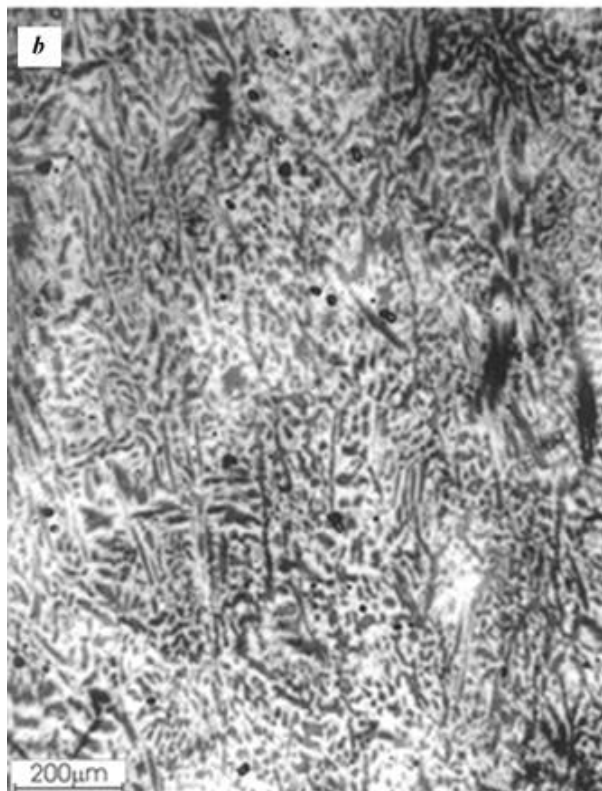
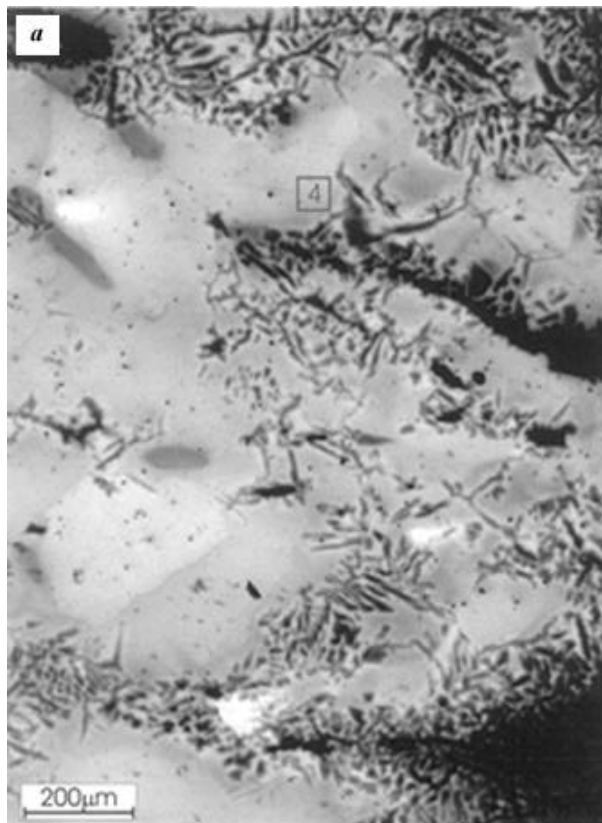


**Figure 4 a-b.** Microstructures of matrix region revealed using Klemm etchant.

that the precipitation of austenite took place along the grain boundaries as allotriomorphs, and additionally grew into the ferrite grains in a needle-shaped morphology. On cooling the material, the austenite transforms to ferrite by massive transformation, thereby not allowing redistribution of the segregated P at high temperature<sup>13,14</sup>. Microsegregation of P occurs during this transformation because the solubility of P is higher in ferrite than in austenite. Although the room-temperature phase is completely ferrite (for example, the entire microstructure in Figure 4 a and b), the Klemm etchant reveals microsegregation of P at grain boundaries. The prior austenite locations are revealed in darker contrast (i.e. lower P content) and therefore, the Klemm etchant can also be utilized to understand the high-temperature ferrite–austenite (and also austenite–ferrite) transformations, like the Oberhoffer etchant. For example, austenite has nucleated and grown from the ferrite grain boundaries as allotriomorphs and needles (Figure 4 a), which can also be visualized in the sample etched with Oberhoffer reagent (Figure 1 b). Interestingly, the growth morphology of austenite at high temperature, as revealed by the etch, conforms to earlier observations of high temperature ferrite–austenite transformations in Fe–P alloys<sup>13,14</sup>. The inhomogeneity in P concentration in the matrix is also revealed in Figure 4 b, which shows the matrix at another location. This microstructure is indicative of the iron having received a heat treatment in the dual phase (austenite + ferrite) region, thereby resulting in the formation of austenite (its ghost structure revealed as dark regions in Figure 4 b). The treatment times must not have been long because spheroidization of the austenite needles is not noticed in Figure 4 b. Moreover, as the prior phase boundaries are etched clearly, it indicates that the cooling rate after the high-temperature treatment must have been fast, thereby retaining P segregation. These examples illustrate that the Klemm etchant can be used to reveal the non-uniform compositional distribution of P in ancient iron. It is important to emphasize that the microstructures in the iron at room temperature were fully ferritic when examined. The Klemm etchant reveals the P inhomogeneities remaining from the dual phase structure at high temperatures.

In summary, the usefulness of utilizing Klemm etchant for revealing the non-homogeneous distribution of P in ancient archaeological iron by colour metallography has been demonstrated. Apart from revealing regions of low and high P content, the etchant is also capable of revealing 'ghost' structures in archaeological irons.

1. Kumar, V. and Balasubramaniam, R., On the origin of high phosphorus content in ancient Indian iron. *Int. J. Met. Mater. Processes*, 2002, **14**, 1–14.
2. McDonnell, G., *World Archaeol.*, 1989, **20**, 373–382.
3. Dillmann, P. and Balasubramaniam, R., Characterization of ancient Indian iron and entrapped slag inclusions, electron, photon and nuclear microprobes. *Bull. Mater. Sci.*, 2001, **24**, 317–322.
4. Dube, R. K., Aspects of powder technology in ancient and medieval India. *Powder Metall.*, 1990, **33**, 119–125.
5. Ramesh Kumar, A. V. and Balasubramaniam, R., Corrosion product analysis of ancient corrosion resistant Indian iron. *Corros. Sci.*, 1998, **40**, 1169–1178.
6. Balasubramaniam, R., On the corrosion resistance of the Delhi iron pillar. *Corros. Sci.*, 2000, **42**, 2103–2129.
7. Misawa, T., Kyuno, T., Suetaka, W. and Shimodaira, S., The mechanism of atmospheric rusting and the effect of Cu and P on the rust formation of low alloy steels. *Corros. Sci.*, 1971, **11**, 35–48.
8. Yamashita, M., Miyuki, H., Matsuda, Y., Nagano, H. and Misawa, T., The Long Term Growth of the Protective Rust Layer Formed on Weathering Steel by Atmospheric Corrosion During a Quarter of a Century. *Corros. Sci.*, 1994, **36**, 283–299.
9. Hadfield, R., Sinhalese iron and steel of ancient origin. *J. Iron Steel Inst.*, 1912, **85**, 134–174.
10. Gouthama and Balasubramaniam, R., Alloy design of ductile phosphoric iron: ideas from archaeometallurgy. *Bull. Mater. Sci.*, 2003, **26**, 483–492.
11. Vizcaino, A., Budd, P. and McDonnell, J. G., An experimental investigation of the behaviour of phosphorus in bloomery iron. *Bull. Mater. Mus.*, 1998, **29**, 13–19.
12. Vizcaino, A., McColm, I. J. and McDonnell, J. G., A thermal analysis study of the role of phosphates in the 'Bloomery' iron process. *Bull. Mater. Mus.*, 1998, **30**, 38–51.
13. Stewart, J. W., Charles, J. A. and Wallach, E. R., Iron–Phosphorus carbon system. Part 3: metallography of low carbon iron–phosphorus alloys. *Mater. Sci. Technol.*, 2000, **16**, 291–303.
14. Stewart, J. W., Charles, J. A. and Wallach, E. R., Iron–Phosphorus carbon system. Part 2: metallographic behaviour of Oberhoffer's reagent. *Mater. Sci. Technol.*, 2000, **16**, 283–290.
15. Thomsen, R., *J. Iron Steel Inst.*, 1966, **204**, 905–909.
16. Piaskowski, J., *Archaeometals*, 1989, **3**, 47–59.
17. Piaskowski, J., *Z. Archaeol.*, 1989, **18**, 213–226.
18. Stewart, J., The metallurgy and metallography of archaeological iron, Ph D thesis, University of Cambridge, 1997.
19. Vats, M. S., The Gupta temple at Deogarh. *Mem. Archaeol. Surv. India*, 1952.
20. Harle, J. C., *Gupta Sculpture: Indian Sculpture of the Fourth to the Sixth Centuries AD*, Clarendon Press, Oxford, 1974.
21. Puri, V., Balasubramaniam, R. and Ramesh Kumar, A. V., Corrosion behaviour of ancient 1500-year old Gupta iron. *Bull. Met. Mus.*, 1997, **28**, 1–10.
22. Balasubramaniam, R., A new study of the Dhar iron pillar. *Indian J. Hist. Sci.*, 2002, **37**, 115–151.

ACKNOWLEDGEMENT. We thank the Archaeological Survey of India for assistance.

Received 27 January 2003; revised accepted 12 July 2004